Electronic Supplementary Material (ESI) for Journal of Materials Chemistry C.

Supporting Information

Optimize and Expand the Schiff Base [Zn-Dy] Unit to Enhance the Performance of Single Molecule Magnetic Materials

Zhi-Ying Zhao[a], Hao-Hang Xu[b], Peng Chen[a], Yu-Xin Li[a], Yu Sui*[b], Wen-Bin Sun*[a]

a. Key Laboratory of Functional Inorganic Material Chemistry Ministry of Education, School of Chemistry and Material Science Heilongjiang University, 74 Xuefu Road, Harbin 150080, P. R. China.

b. School of Physics, Harbin Institute of Technology, Harbin 150001, P. R. China.

E-mail: wenbinsun@126.com

E-mail: suiyu@hit.edu.cn

Table S1 Crystallographic data for **1-5**

	1	**2**	**3**	**4**	**5**
Empirical formula	$C_{37}H_{37}DyF_6N_3O_8PZn$	$C_{37}H_{38}DyF_6N_4O_8PZn$	$C_{80}H_{86}Dy_2F_{12}N_6O_{16}P_2Zn_2$	$C_{68}H_{76}Dy_2F_{12}N_6O_{16}P_2Zn_2$	$C_{70}H_{78}Dy_2F_{12}N_6O_{16}P_2Zn_2$
FW (g mol^{-1})	1024.54	1038.55	2133.22	1979.03	2005.06
Crystal system	Monoclinic	Monoclinic	Monoclinic	triclinic	triclinic
Space group	*P*21/n	*P*21/n	*P*21/n	P-1	P-1
Temperature (K)	293(2)	293(2)	293(2)	298	296
a (Å)	9.9785(6)	9.8769(6)	9.9515(7)	10.7206(5)	10.411(3)
b (Å)	25.7192(10)	25.9707(17)	25.9689(18)	12.2311(7)	12.658(3)
c (Å)	16.1066(12)	16.2390(13)	16.5554(10)	15.8508(9)	16.294(4)
α (°)	90.00	90.00	90.00	73.483(5)	106.985(2)
β (°)	103.364(6)	103.348(7)	100.118(6)	89.759(4)	95.584(3)
γ (°)	90.00	90.00	90.00	86.099(4)	95.855(3)
V ($Å^3$)	4021.7(4)	4052.9(5)	4211.9(5)	1987.80(19)	2024.7(8)
ρ_{cacd} (Mg cm^{-3})	1.692	1.702	1.682	1.653	1.644
μ (mm^{-1})	2.561	2.543	2.449	2.587	2.541
F (000)	2036.0	2064.0	2132.0	984.0	998.0
Collected reflections	40932	24794	13728	14863	13479
Independent reflections	9207	8235	8217	9922	6878
Rint	0.1000	0.1006	0.1150	0.0288	0.0304
R1 [I > 2σ(I)]	0.1259	0.0835	0.0907	0.0617	0.0503
wR2 (all data)	0.2443	0.2202	0.2638	0.2046	0.1508
Goodness of fit on F^2	1.293	1.040	0.970	1.110	1.024

Table S2 Selected bond bengths (Å) and Angles (°) for **1**.

Dy1-Zn1	3.4395(16)	Dy1-O7	2.298(11)
Dy1-O2	2.362(9)	Dy1-O8	2.213(11)
Dy1-O6	2.242(10)	Zn1-O2	1.988(9)
Dy1-O5	2.272(11)	Zn1-O3	2.003(9)
Dy1-O3	2.331(9)	Zn1-N1	2.013(11)
Dy1-O4	2.593(10)	Zn1-N2	2.026(11)
Dy1-O1	2.614(10)	Zn1-N3	2.060(14)
O2-Dy1-Zn1	34.1(2)	O3-Dy1-O4	62.6(3)
O2-Dy1-O4	126.7(3)	O3-Dy1-O1	125.1(3)
O2-Dy1-O1	62.0(3)	O4-Dy1-Zn1	96.9(2)
O6-Dy1-Zn1	170.7(3)	O4-Dy1-O1	149.3(3)
O6-Dy1-O2	144.6(4)	O1-Dy1-Zn1	96.0(2)
O6-Dy1-O5	76.1(4)	O7-Dy1-Zn1	99.4(3)
O6-Dy1-O3	140.8(4)	O7-Dy1-O2	122.4(4)
O6-Dy1-O4	79.3(4)	O7-Dy1-O3	87.4(4)
O6-Dy1-O1	83.5(4)	O7-Dy1-O4	68.9(4)
O6-Dy1-O7	87.2(4)	O7-Dy1-O1	135.6(4)
O5-Dy1-Zn1	94.8(3)	O8-Dy1-Zn1	92.4(4)
O5-Dy1-O2	85.3(4)	O8-Dy1-O2	77.4(4)
O5-Dy1-O3	87.3(4)	O8-Dy1-O6	95.8(5)
O5-Dy1-O4	79.0(4)	O8-Dy1-O5	136.8(4)
O5-Dy1-O1	72.3(4)	O8-Dy1-O3	119.6(4)
O5-Dy1-O7	146.1(4)	O8-Dy1-O4	142.1(4)
O3-Dy1-Zn1	34.3(2)	O8-Dy1-O1	64.7(4)
O3-Dy1-O2	66.1(3)	O8-Dy1-O7	73.3(4)

Table S3 Selected bond bengths (Å) and Angles (°) for **2**.

Dy1-Zn1	3.4369(14)	Dy1-O7	2.301(8)
Dy1-O3	2.324(6)	Dy1-O8	2.301(9)
Dy1-O2	2.331(7)	Zn1-O3	1.995(7)
Dy1-O4	2.597(7)	Zn1-O2	1.995(7)
Dy1-O1	2.615(8)	Zn1-N3	2.036(10)
Dy1-O5	2.273(8)	Zn1-N2	2.033(9)
Dy1-O6	2.254(8)	Zn1-N1	2.034(10)
O3-Dy1-Zn1	34.07(16)	O6-Dy1-O3	141.4(3)
O3-Dy1-O2	65.7(2)	O6-Dy1-O2	144.9(3)
O3-Dy1-O4	62.3(2)	O6-Dy1-O4	80.2(3)
O3-Dy1-O1	124.5(2)	O6-Dy1-O1	83.5(3)
O2-Dy1-Zn1	34.12(16)	O6-Dy1-O5	75.0(3)

O2-Dy1-O4	126.2(2)	O6-Dy1-O7	89.1(3)
O2-Dy1-O1	62.0(2)	O6-Dy1-O8	93.2(3)
O4-Dy1-Zn1	96.33(17)	O7-Dy1-Zn1	96.8(2)
O4-Dy1-O1	149.2(3)	O7-Dy1-O3	86.1(3)
O1-Dy1-Zn1	96.13(17)	O7-Dy1-O2	120.1(3)
O5-Dy1-Zn1	96.97(19)	O7-Dy1-O4	69.4(2)
O5-Dy1-O3	87.7(3)	O7-Dy1-O1	136.4(3)
O5-Dy1-O2	87.8(3)	O7-Dy1-O8	71.3(3)
O5-Dy1-O4	77.5(3)	O8-Dy1-Zn1	94.2(3)
O5-Dy1-O1	73.0(3)	O8-Dy1-O3	121.0(3)
O5-Dy1-O7	145.3(3)	O8-Dy1-O2	79.7(3)
O5-Dy1-O8	138.8(3)	O8-Dy1-O4	140.2(3)
O6-Dy1-Zn1	171.7(2)	O8-Dy1-O1	66.4(3)

Table S4 Selected bond bengths (Å) and Angles (°) for **3**.

Dy1-Zn1	3.422(2)	Dy1-O2	2.332(10)
Dy1-O6	2.247(11)	Dy1-O7	2.278(13)
Dy1-O3	2.308(11)	Zn1-N1	2.054(13)
Dy1-O4	2.617(11)	Zn1-O3	2.004(11)
Dy1-O8	2.310(12)	Zn1-N3	2.055(12)
Dy1-O1	2.624(12)	Zn1-N2	2.035(13)
Dy1-O5	2.322(12)	Zn1-O2	1.988(10)
O6-Dy1-O7	91.1(4)	O8-Dy1-O4	136.4(4)
O6-Dy1-O3	144.3(4)	O5-Dy1-O4	72.5(4)
O7-Dy1-O3	79.4(4)	O2-Dy1- O4	124.1(4)
O6-Dy1-O8	91.3(4)	O6-Dy1-O1	81.5(4)
O7-Dy1-O8	72.0(4)	O7-Dy1-O1	141.2(4)
O3-Dy1-O8	117.5(4)	O3-Dy1-O1	126.4(4)
O6-Dy1-O5	75.1(4)	O8-Dy1-O1	70.2(4)
O7-Dy1-O5	136.7(5)	O5-Dy1-O1	78.0(4)
O3-Dy1-O5	88.4(4)	O2-Dy1-O1	61.6(3)
O8-Dy1-O5	147.0(4)	O4-Dy1-O1	149.3(4)
O6-Dy1-O2	141.7(4)	O6-Dy1-Zn1	172.2(3)
O7-Dy1-O2	123.6(4)	O7-Dy1-Zn1	95.6(3)
O3-Dy1- O2	66.1(4)	O3-Dy1-Zn1	34.5(3)
O8-Dy1- O2	85.6(4)	O8-Dy1- Zn1	94.6(3)
O5-Dy1-O2	87.1(4)	O5-Dy1- Zn1	97.2(3)
O6-Dy1-O4	82.8(4)	O2-Dy1- Zn1	34.2(2)
O7-Dy1-O4	65.0(4)	O4-Dy1- Zn1	96.4(3)
O3-Dy1-O4	61.9(4)	O1-Dy1- Zn1	95.7(3)

Table S5 Selected bond bengths (Å) and Angles (°) for **4**.

Dy1-Zn1	3.4884(8)	Dy1-O8	2.304(6)
Dy1-O3	2.320(5)	Dy1-O7	2.292(6)
Dy1-O2	2.321(4)	Zn1-O3	2.057(5)
Dy1-O5	2.323(5)	Zn1-O2	2.041(5)
Dy1-O6	2.269(5)	Zn1-N3	2.126(6)
Dy1-O4	2.575(5)	Zn1-N1	2.057(6)
Dy1-O1	2.522(5)	Zn1-N2	2.049(6)
O3-Dy1-Zn1	34.63(12)	O6-Dy1-O8	94.1(2)
O3-Dy1-O2	66.37(17)	O6-Dy1-O7	93.6(2)
O3-Dy1-O5	83.22(19)	O4-Dy1-Zn1	98.85(13)
O3-Dy1-O4	64.22(18)	O1-Dy1-Zn1	98.65(12)
O3-Dy1-O1	127.84(17)	O1-Dy1-O4	145.74(19)
O2-Dy-Zn1	34.21(11)	O8-Dy1-Zn1	96.32(16)
O2-Dy-O5	86.62(18)	O8-Dy1-O3	119.7(2)
O2-Dy-O4	127.76(17)	O8-Dy1-O2	82.03(19)
O2-Dy-O1	64.43(16)	O8-Dy1-O5	146.6(2)
O5-Dy1-Zn1	93.64(13)	O8-Dy1-O4	138.2(2)
O5-Dy1-O4	72.0(2)	O8-Dy1-O1	69.0(2)
O5-Dy1-O1	77.73(19)	O7-Dy1-Zn1	95.69(17)
O6-Dy1-Zn1	169.03(15)	O7-Dy1-O3	82.2(2)
O6-Dy1-O3	142.1(2)	O7-Dy1-O2	121.3(2)
O6-Dy1-O2	141.0(2)	O7-Dy1-O5	139.0(2)
O6-Dy1-O5	75.5(2)	O7-Dy1-O4	67.2(2)
O6-Dy1-O4	79.4(2)	O7-Dy1-O1	139.3(2)
O6-Dy1-O1	77.86(19)	O7-Dy1-O8	72.2(2)

Table S6 Selected bond bengths (Å) and Angles (°) for **5**.

Dy1-Zn1	3.488(11)	Dy1-O8	2.286(6)
Dy1-O3	2.338(5)	Dy1-O7	2.247(8)
Dy1-O2	2.353(5)	Zn1-O3	2.016(4)
Dy1-O5	2.337(5)	Zn1-O2	2.076(5)
Dy1-O4	2.565(6)	Zn1-N3	2.058(5)
Dy1-O1	2.548(8)	Zn1-N2	2.043(6)
Dy1-O6	2.253(6)	Zn1-N1	2.053(6)
O3-Dy1-Zn1	33.69(11)	O6-Dy1-O5	75.1(2)
O3-Dy1-O2	66.54(17)	O6-Dy1-O4	80.9(2)
O3-Dy1-O4	63.03(17)	O6-Dy1-O1	77.5(3)
O3-Dy1-O1	127.0(2)	O6-Dy1-O8	97.0(2)
O2-Dy1-Zn1	35.30(12)	O8-Dy1-Zn1	92.5(17)

O2-Dy1-O4	123.74(18)	O8-Dy1-O3	115.5(2)
O2-Dy1-O1	62.9(2)	O8-Dy1-O2	82.6(2)
O5-Dy1-Zn1	92.69(13)	O8-Dy1-O5	143.6(3)
O5-Dy1-O3	87.11(8)	O8-Dy1-O4	141.6(3)
O5-Dy1-O2	81.12(18)	O8-Dy1-O1	72.6(3)
O5-Dy1-O4	73.23(19)	O7-Dy1-Zn1	95.0(2)
O5-Dy1-O1	71.0(2)	O7-Dy1-O3	78.9(3)
O4-Dy-Zn1	96.43(13)	O7-Dy1-O2	123.8(2)
O1-Dy-Zn1	98.15(18)	O7-Dy1-O5	141.3(3)
O1-Dy-O4	141.8(2)	O7-Dy1-O4	68.3(2)
O6-Dy1-Zn1	167.74(17)	O7-Dy1-O1	144.3(3)
O6-Dy1-O3	143.2(2)	O7-Dy1-O6	95.1(3)
O6-Dy1-O2	138.6(2)	O7-Dy1-O8	73.8(3)

Table S7 Continuous Shape Measures (CShMs) of the coordination geometry for Dy(III) ion in compounds **1**-**5** (S values calculated with the Shape program). The *S* values indicated the proximity to the ideal polyhedron, thus, a *S* = 0 corresponds to the non-distorted polyhedron. The three closer ideal geometry to the real complexes are listed and below is the symmetry and description for each polyhedron.

Complexes	S	polyhedron
1	2.479	JBTPR-8 C_{2v} Biaugmented trigonal prism J50
	2.602	BTPR-8 C_{2v} Biaugmented trigonal prism
	3.774	TDD-8 D_{2d} Triangular dodecahedron
2	2.561	JBTPR-8 C_{2v} Biaugmented trigonal prism J50
	2.640	BTPR-8 C_{2v} Biaugmented trigonal prism
	4.177	TDD-8 D_{2d} Triangular dodecahedron
3	2.610	JBTPR-8 C_{2v} Biaugmented trigonal prism J50
	2.724	BTPR-8 C_{2v} Biaugmented trigonal prism
	4.046	TDD-8 D_{2d} Triangular dodecahedron
4	2.013	BTPR-8 C_{2v} Biaugmented trigonal prism
	2.128	JBTPR-8 C_{2v} Biaugmented trigonal prism J50
	3.560	TDD-8 D_{2d} Triangular dodecahedron
5	2.014	BTPR-8 C_{2v} Biaugmented trigonal prism
	2.082	JBTPR-8 C_{2v} Biaugmented trigonal prism J50
	2.971	TDD-8 D_{2d} Triangular dodecahedron

Table S8. The dihedral angle β between planes (one plane composed of N2O2 and another is the hard-plane, Fig. S3) of complexes **1**–**5**.

Complexes	1	2	3	4	5
β (°)	10.902	10.824	9.207	3.901	14.303

Table S9. The distance of Zn between plane of complexes **1**–**5.**

Complexes	1	2	3	4	5
Plane	O2, O3, N1, N2,	O2, O3, N1, N2,	O2, O3, N1, N2,	O2, O3, N1, N2,	O2, O3, N1, N2,
***d*(Zn-Plane)(**Å)	0.542	0.565	0.532	0.355	0.108

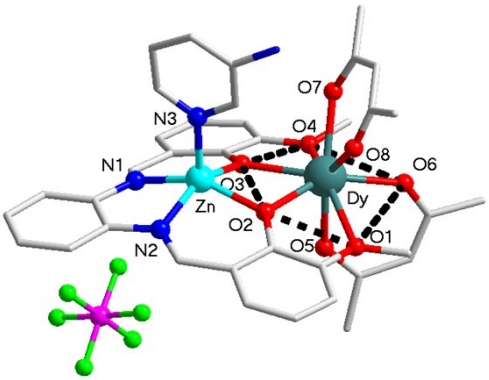

Fig. S1 Molecular structures of **2** Color code: Dy (teal), O (red), Zn (turquoise), F (green), C (grey), N (blue), Black dotted line is $Plane_{O5}$. H atoms were omitted for clarity.

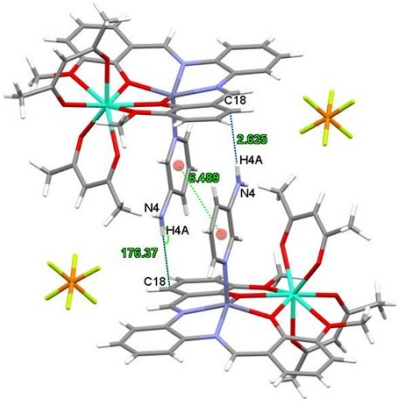

Fig. S2 Intermolecular hydrogen bonding and Π-Π conjugate effect between molecules for complex **2.**

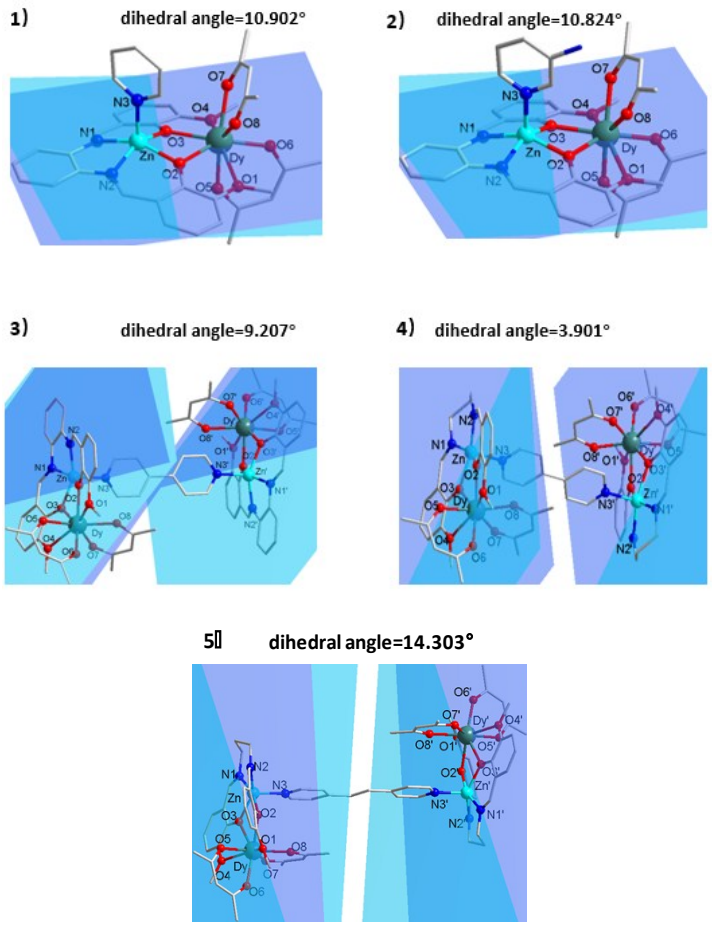

Fig. S3 The dihedral angle between the hard-plane and plane of N2O2 in **1**–**5**.

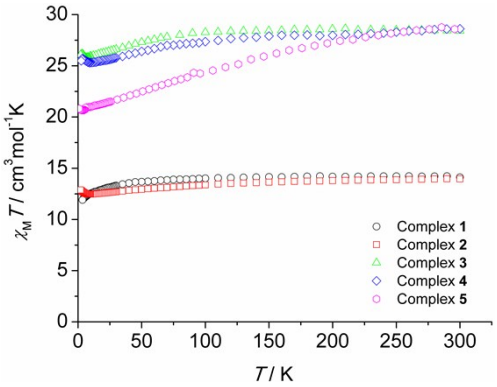

Fig. S4 experimental data of temperature dependence of the $\chi_M T$ values of complexes **1**-**5.**

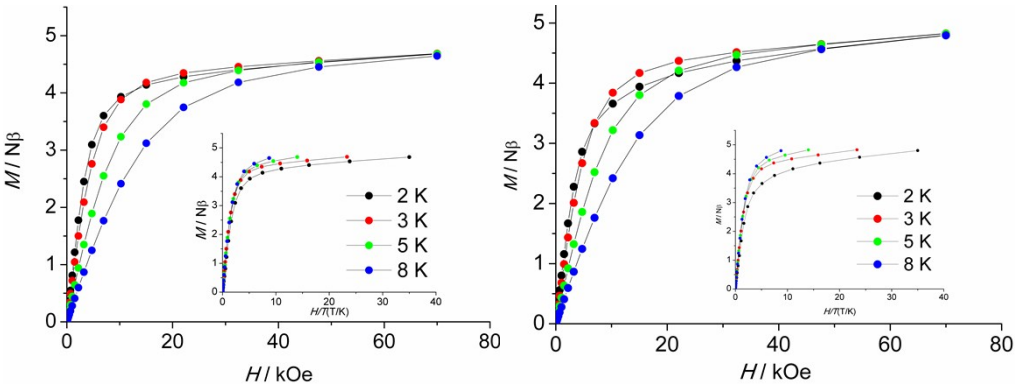

Fig. S5 Field dependence of the magnetization between 2 and 8 K for **1**(left) and **2**(right).

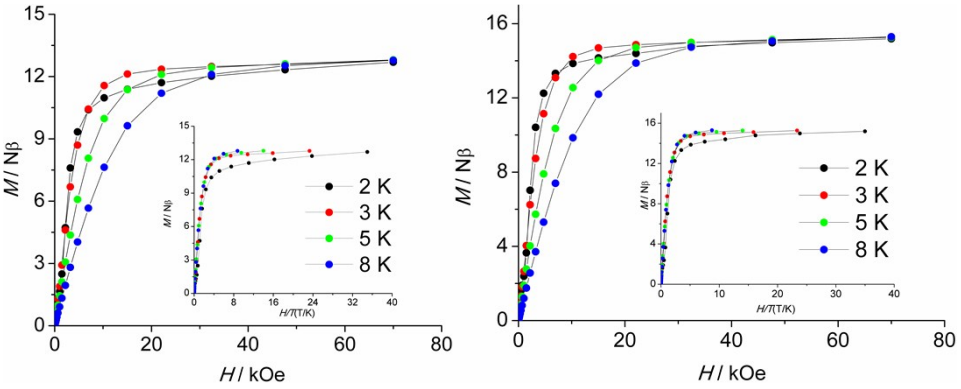

Fig. S6 Field dependence of the magnetization between 2 and 8 K for **3**(left) and **4**(right).

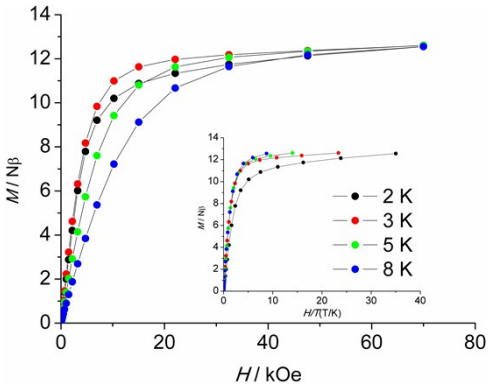

Fig. S7 Field dependence of the magnetization between 2 and 8 K for **5**.

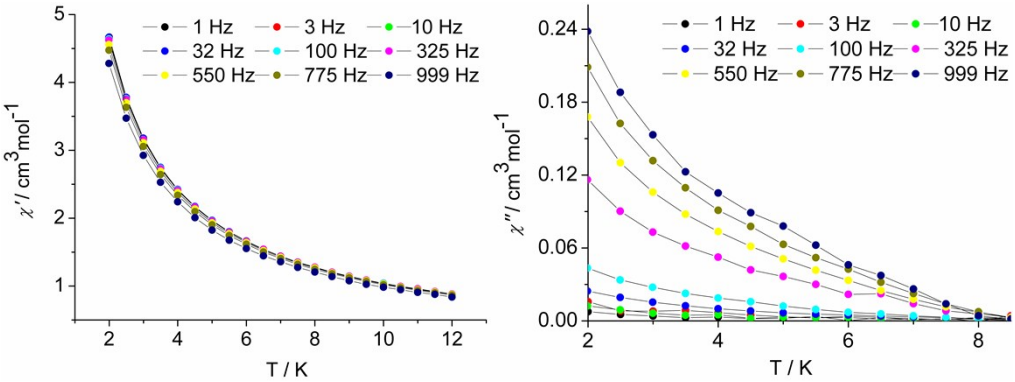

Fig. S8 The temperature dependence of the in-phase (χ', left) and the out-of-phase (χ'', right) ac susceptibility component under zero field for complex **1.**

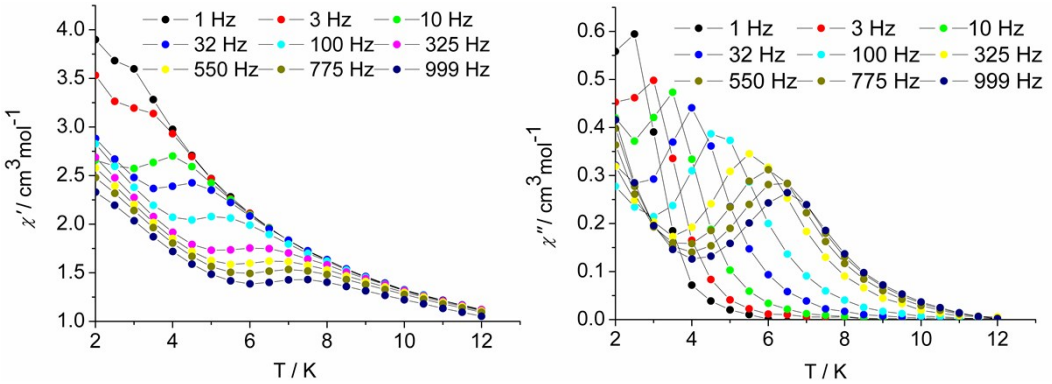

Fig. S9 The temperature dependence of the in-phase (χ', left) and the out-of-phase (χ'', right) ac susceptibility component under 1500 Oe or complex **1.**

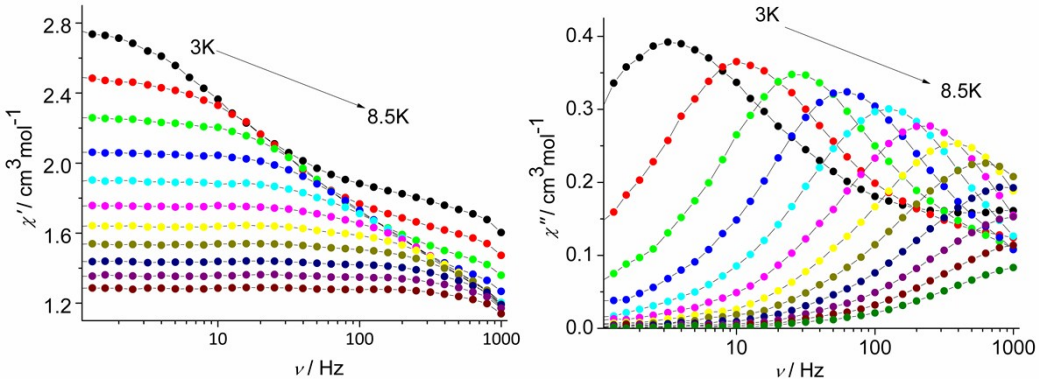

Fig. S10 The frequency dependence of the in-phase (χ', left) and the out-of-phase (χ'', right) ac susceptibility component under 1500 Oe for complex **1.**

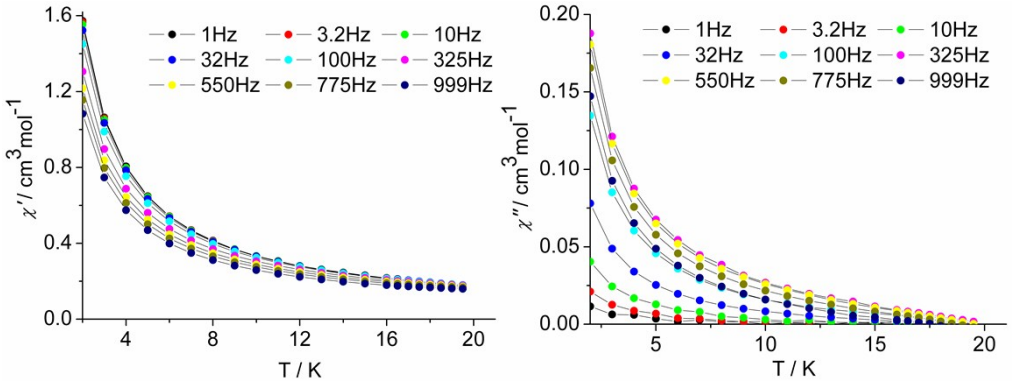

Fig. S11 The temperature dependence of the in-phase (χ', left) and the out-of-phase (χ'', right) ac susceptibility component under zero field for complex **2.**

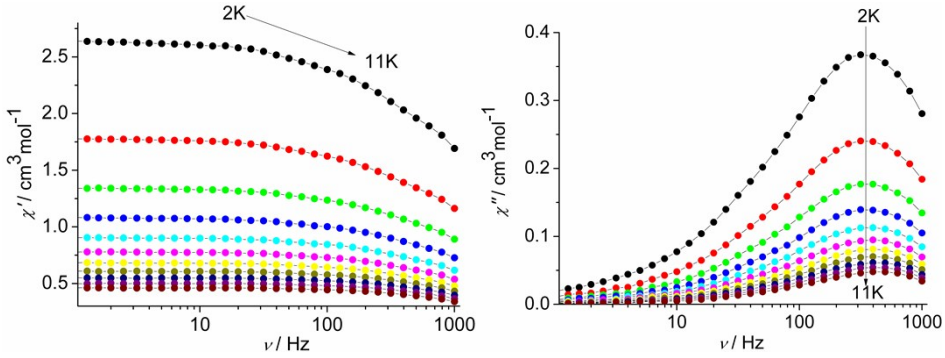

Fig. S12 The frequency dependence of the in-phase (χ', left) and the out-of-phase (χ'', right) ac susceptibility component under zero field for complex **2.**

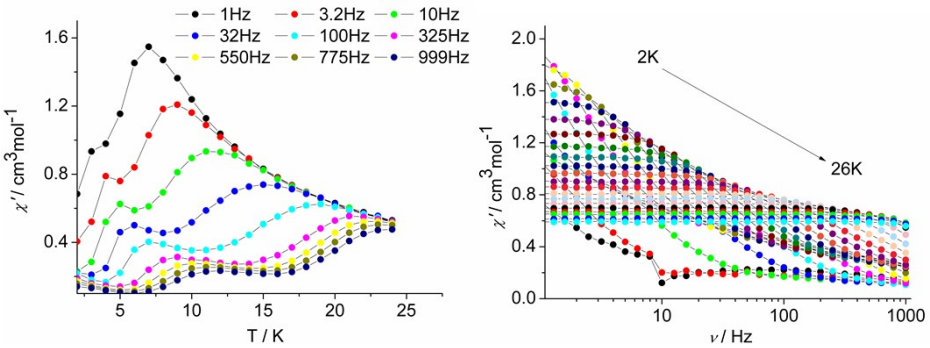

Fig. S13 The temperature dependence of the in-phase (χ', left) and the in-phase (χ', right) ac susceptibility component under 1500 Oe for complex **1-2.**

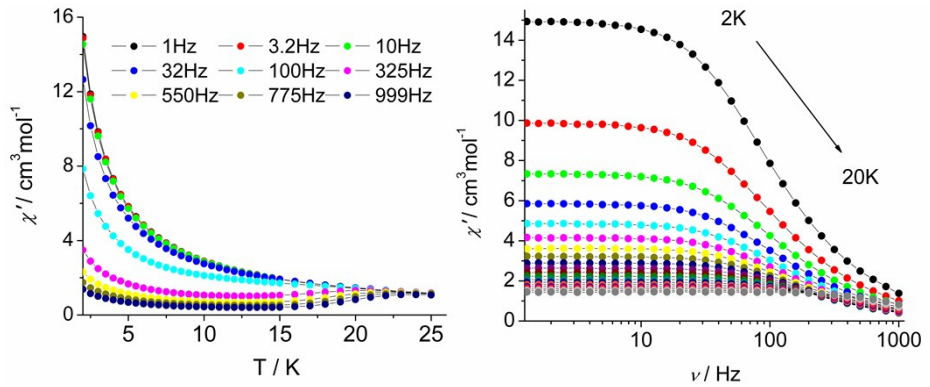

Fig. S14 The temperature dependence of the in-phase (χ', left) and the frequency dependence of the in-phase (χ', right) ac susceptibility component under zero field for complex **3.**

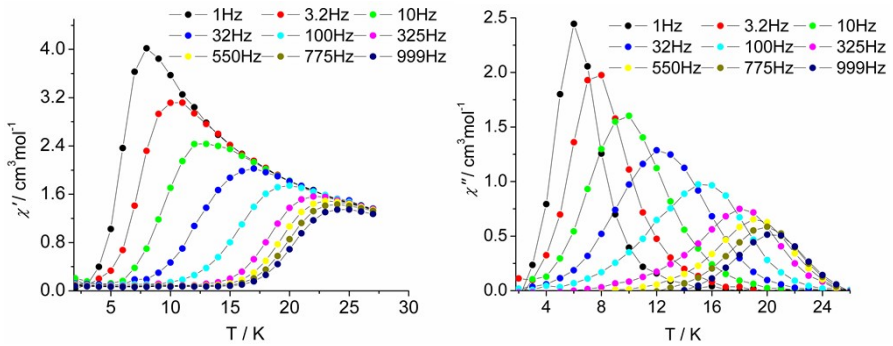

Fig. S15 The temperature dependence of the in-phase (χ', left) and the out-of-phase (χ'', right) ac susceptibility component under 1500 Oe for complex **3.**

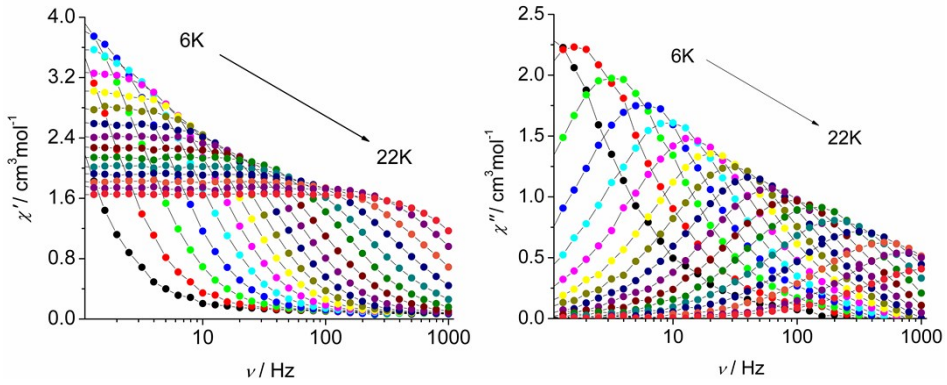

Fig. S16 The frequency dependence of the in-phase (χ', left) and the out-of-phase (χ'', right) ac susceptibility component under 1500 Oe or complex **3.**

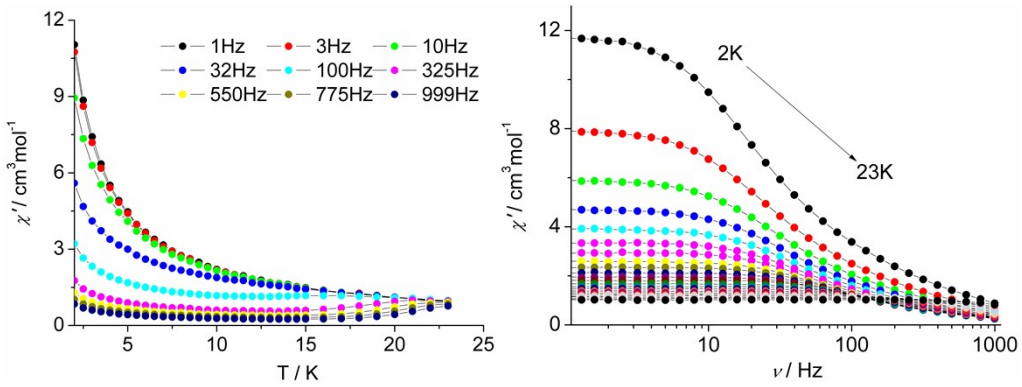

Fig. S17 The temperature dependence of the in-phase (χ', left) and the frequency dependence of the in-phase (χ', right) ac susceptibility component under zero field for complex **4.**

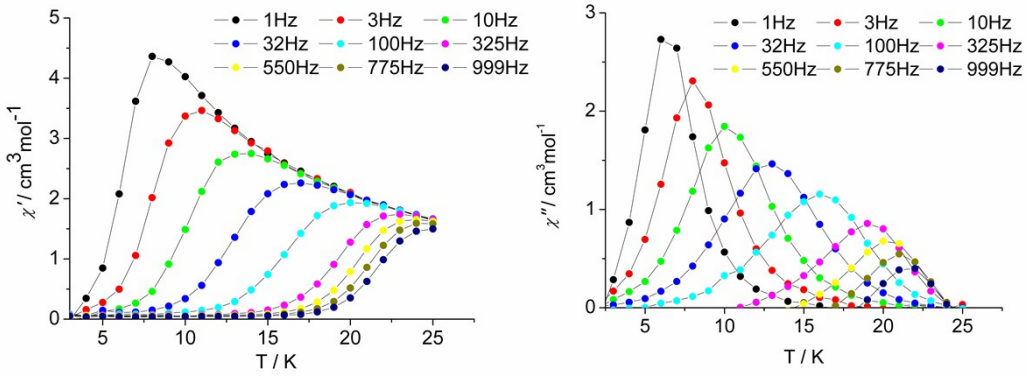

Fig. S18 The temperature dependence of the in-phase (χ', left) and the out-of-phase (χ'', right) ac susceptibility component under 1500 Oe for complex **4.**

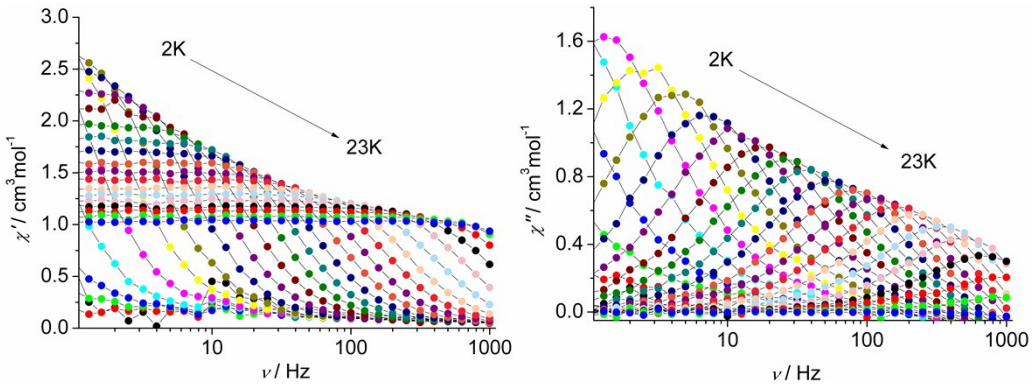

Fig. S19 The frequency dependence of the in-phase (χ', left) and the out-of-phase (χ'', right) ac susceptibility component under 1500 Oe or complex **4.**

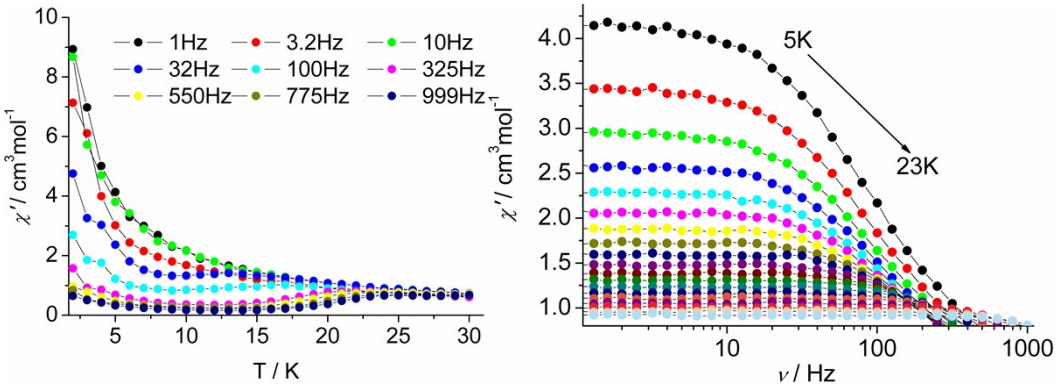

Fig. S20 The temperature dependence of the in-phase (χ', left) and the frequency dependence of the in-phase (χ', right) ac susceptibility component under zero field for complex **5**.

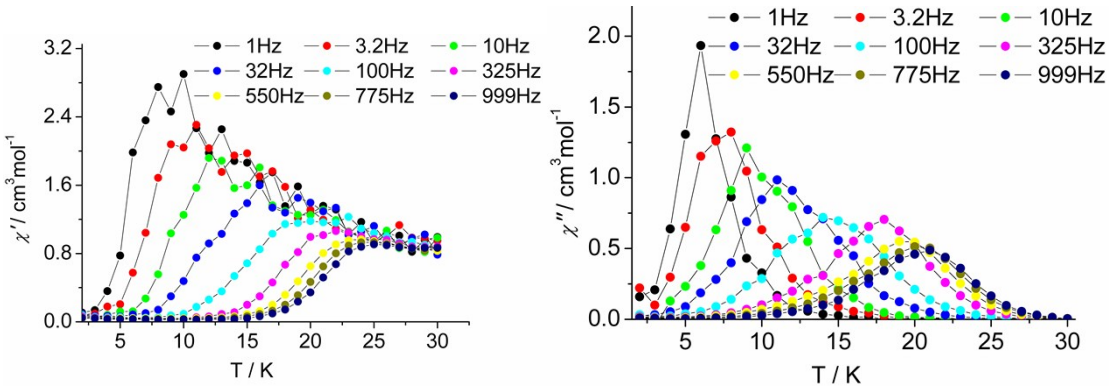

Fig. S21 The temperature dependence of the in-phase (χ', left) and the out-of-phase (χ'', right) ac susceptibility component under 1500 Oe for complex **5**.

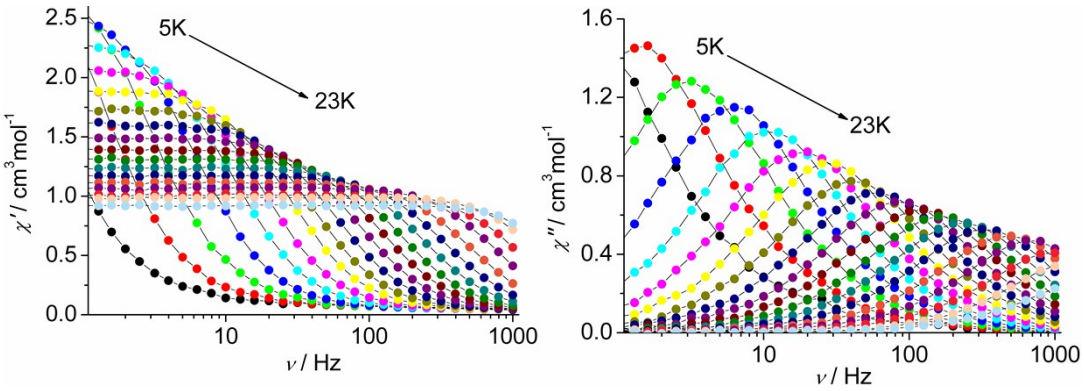

Fig. S22 The frequency dependence of the in-phase (χ', left) and the out-of-phase (χ'', right) ac susceptibility component under 1500 Oe or complex **5.**

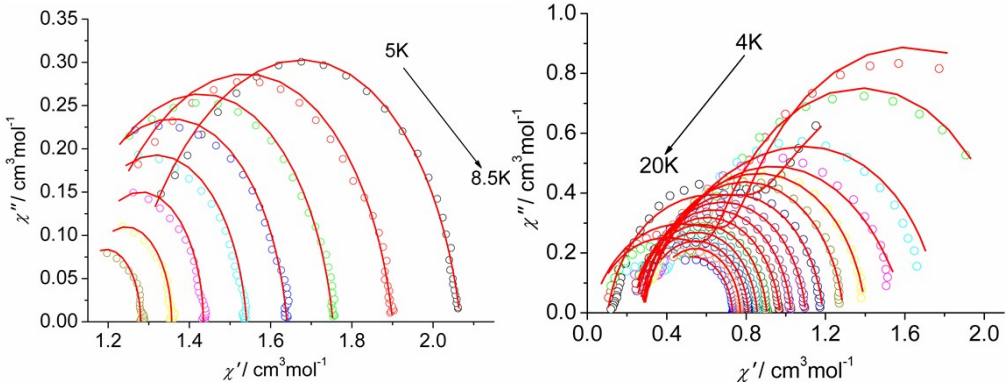

Fig. S23 Cole-Cole (Argand) plot for **1** (left) and **2** (right) obtained using the ac susceptibility data. The solid lines correspond to the best fit obtained with a generalized Debye model under 1500 Oe.

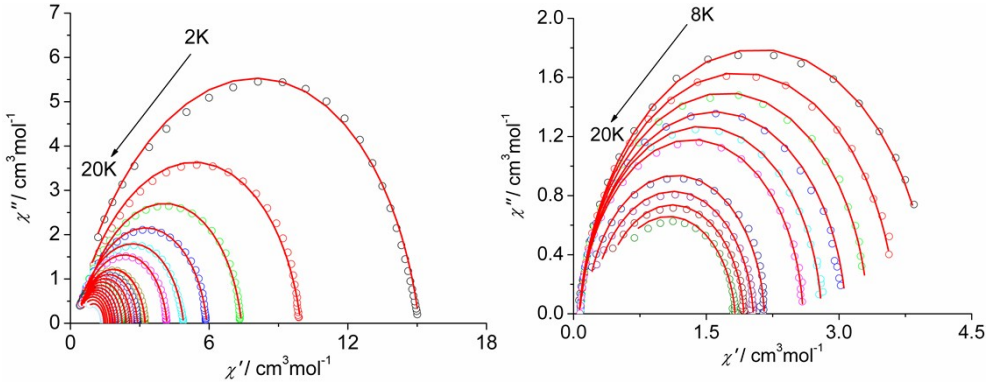

Fig. S24 Cole-Cole (Argand) plot for **3** obtained using the ac susceptibility data. The solid lines correspond to the best fit obtained with a generalized Debye model under zero field (left) and under 1500 Oe (right).

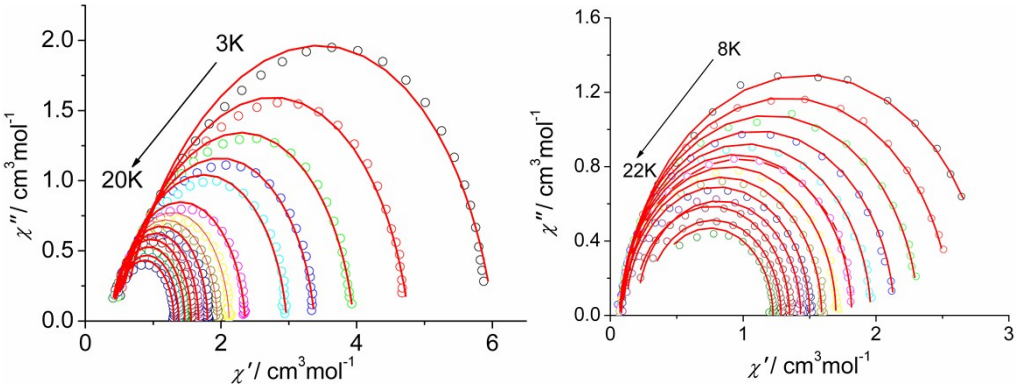

Fig. S25 Cole-Cole (Argand) plot for **4** obtained using the ac susceptibility data. The solid lines correspond to the best fit obtained with a generalized Debye model under zero field (left) and under 1500 Oe (right).

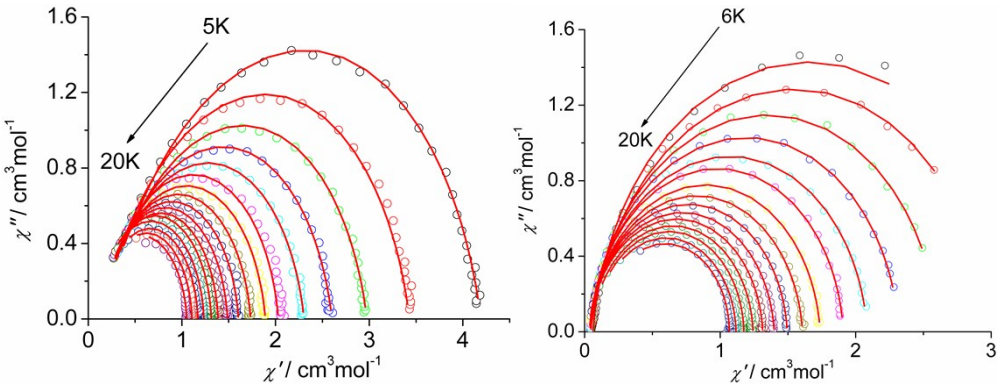

Fig. S26 Cole-Cole (Argand) plot for **5** obtained using the ac susceptibility data. The solid lines correspond to the best fit obtained with a generalized Debye model under zero field (left) and under 1500 Oe (right).

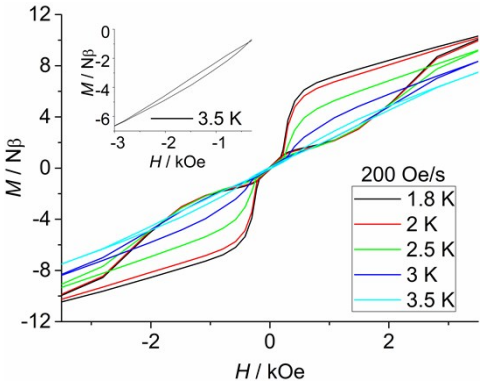

Fig. S27 Field dependence of magnetization of samples **3** between 1.8 K and 3.5 K at a sweep rate of 200 Oe s^{-1}

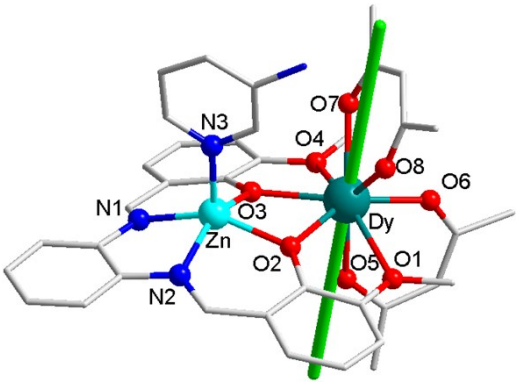

Fig. 28 The orientation of the local main magnetic axes of the ground Kramers doublet on Dy(III) of complex **2**.

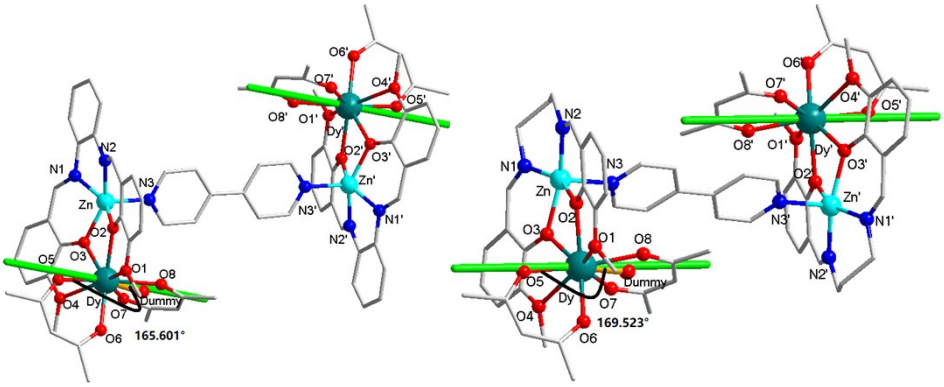

Fig. S29 The angle of O_{Dummy}-Dy-O5 of complexes **3**-**4.**

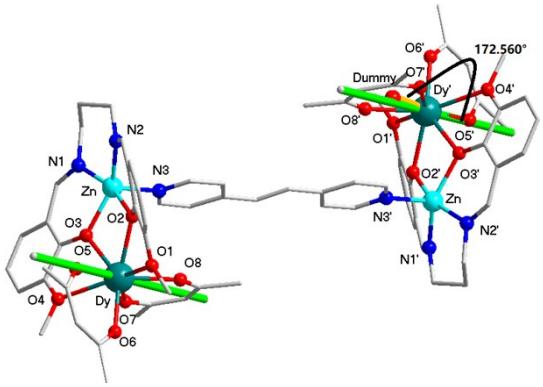

Fig. S30 The angle of O_{Dummy}-Dy-O5 of complex **5.**

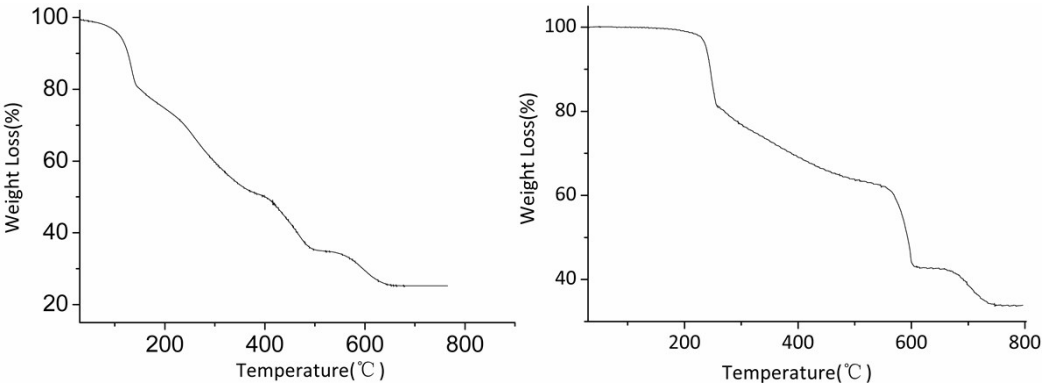

Fig. S31 TG curves of complexes **3** and **4**.

Crystals of **3** have been selected for the thermogravimetric analysis in the experimental range of 30–780 degree. A total weight loss of 74.10 wt% (calcd. 74.22 wt%) is found. The initial stage is owing to the removal of one *n*-hexane molecule (found 3.64 wt%, calcd. 4.04 wt%) before 105 degree, in accordance with the electron counts obtained from SQUEEZE.

Crystals of **4** have been selected for the thermogravimetric analysis in the experimental range of 30–780 degree. A total weight loss of 72.66 wt% (calcd. 72.34 wt%) is found. But no solvent evolution was found around 100 degree.

Table S10. Best fitted parameters (χ_T, χ_S, τ and α) with the extended Debye model for complex **1** at 1500 Oe in the temperature range 5-8.5 K.

T/ K	χ_S / cm^3 mol^{-1}	χ_T / cm^3 mol^{-1}	τ/s	α
5	1.23377	2.06776	0.00123	0.20013
5.5	1.13034	1.90056	0.00070	0.18524
6	1.06588	1.75348	0.00043	0.16762
6.5	1.04990	1.63994	0.00029	0.14456
7	1.08140	1.54065	0.00025	0.11071
7.5	1.12902	1.43410	0.00023	0.00956
8	1.13320	1.35647	0.00022	0.00986
8.5	1.11146	1.28000	0.00019	0.00376

Table S11. Best fitted parameters (χ_T, χ_S, τ and α) with the extended Debye model for complex **2** at 1500 Oe in the temperature range 5-8.5 K.

T/ K	χ_S / cm^3 mol^{-1}	χ_T / cm^3 mol^{-1}	τ_1/s	α_1	τ_2/s	α_2	β
6	0.02000	2.50000	0.00190	0.23000	0.13101	0.00141	0.31000
7	0.02000	2.12003	0.00089	0.23000	0.06369	0.00243	0.31000
8	0.02001	1.86002	0.00049	0.22999	0.03493	0.00068	0.31000
9	0.27143	1.51000	0.00922	0.23000	0.02726	0.07191	0.49548
10	0.24727	1.37095	0.01111	0.13001	0.00935	0.44000	0.70990
11	0.19401	1.27000	0.00832	0.13001	0.00269	0.44000	0.71000
12	0.25383	1.35406	0.00438	0.13001	0.50485	0.43995	0.71000
13	0.24574	1.23512	0.00308	0.13000	0.50497	0.43994	0.71000
14	0.22613	1.15499	0.00222	0.13001	0.50491	0.43987	0.71000
15	0.21192	1.08150	0.00156	0.13019	0.50488	0.43985	0.71000
16	0.12584	0.86362	0.00128	0.13001	0.00036	0.43754	0.70999
17	0.12584	0.86362	0.00128	0.13001	0.00036	0.43754	0.70999
18	0.22086	0.85571	0.00050	0.13001	0.50479	0.43952	0.70993
19	0.24041	0.76921	0.00034	0.13000	0.50499	0.44000	0.70999
20	0.27599	0.67142	0.00023	0.13000	0.50488	0.44000	0.70998

Table S12. Best fitted parameters (χ_T, χ_S, τ and α) with the extended Debye model for complex **3** at 0 Oe in the temperature range 2-20 K.

T/ K	χ_S / cm^3 mol^{-1}	χ_T / cm^3 mol^{-1}	τ/s	α
2	0.06457	15.09170	0.00156	0.19206
3	0.18411	9.96463	0.00146	0.18617
4	0.42109	7.40004	0.00141	0.16015
5	0.33635	5.90215	0.00132	0.16098
6	0.22603	4.89710	0.00121	0.16589
7	0.33813	4.17962	0.00118	0.13711
8	0.43645	3.22608	0.00106	0.08403
9	0.33571	3.24012	0.00102	0.11169
10	0.32292	2.90615	0.00094	0.10056

11	0.30921	2.64325	0.00086	0.09188
12	0.29064	2.41969	0.00077	0.08434
13	0.31054	2.23424	0.00071	0.06920
14	0.35109	2.06952	0.00064	0.04281
15	0.34492	1.92451	0.00056	0.03348
16	0.27965	1.81580	0.00047	0.05468
17	0.31509	1.70340	0.00040	0.03795
18	0.31924	1.60751	0.00031	0.04732
19	0.42112	1.52363	0.00025	0.02368
20	0.56012	1.44820	0.00022	0.00289

Table S13. Best fitted parameters (χ_T, χ_S, τ and α) with the extended Debye model for complex **3** at 1500 Oe in the temperature range 8-20 K.

T/ K	χ_S / cm^3 mol^{-1}	χ_T / cm^3 mol^{-1}	τ/s	α
8	0.05725	4.64029	0.05159	0.08605
9	0.06275	4.04445	0.02856	0.06725
10	0.06902	3.64505	0.01749	0.05817
11	0.07284	3.32829	0.01144	0.05364
12	0.06443	3.08000	0.00782	0.06170
13	0.07138	2.80363	0.00538	0.04716
14	0.08022	2.59272	0.00374	0.04000
15	0.08442	2.42559	0.00261	0.04290
16	0.24967	2.26130	0.00190	0.00193
17	0.14377	2.15506	0.00116	0.04420
18	0.19796	2.03042	0.00078	0.06341
19	0.28683	1.92397	0.00050	0.06587
20	0.28884	1.82537	0.00029	0.09681

Table S14. Best fitted parameters (χ_T, χ_S, τ and α) with the extended Debye model for complex **4** at 0 Oe in the temperature range 3-22 K.

T/ K	χ_S / cm^3 mol^{-1}	χ_T / cm^3 mol^{-1}	τ/s	α
3	0.49000	8.16524	0.00502	0.24111
4	0.48992	6.02546	0.00418	0.21438
5	0.52259	4.76890	0.00361	0.18003
6	0.47188	3.95568	0.00315	0.16399
7	0.45654	3.38186	0.00281	0.14548
8	0.44519	2.96920	0.00254	0.12065
9	0.43893	2.35999	0.00192	0.02846
10	0.42182	2.35610	0.00202	0.08282
11	0.42148	2.12265	0.00181	0.05991
12	0.42730	1.94505	0.00162	0.03145
13	0.43349	1.80164	0.00135	0.00723
14	0.41586	1.66836	0.00122	0.00031
15	0.39140	1.55932	0.00107	0.00000

16	0.40938	1.46589	0.00089	0.00009
17	0.43952	1.37748	0.00076	0.00017
18	0.43936	1.30475	0.00061	0.00000
19	0.43991	1.23032	0.00047	0.00001
20	0.53929	1.17606	0.00039	0.00011
21	0.43893	2.35999	0.00192	0.02846
22	0.44519	2.96920	0.00254	0.12065

Table S15. Best fitted parameters (χ_T, χ_S, τ and α) with the extended Debye model for complex **4** at 1500 Oe in the temperature range 8-22 K

T/ K	χ_S / cm^3 mol^{-1}	χ_T / cm^3 mol^{-1}	τ/s	α
8	0.09026	3.14980	0.06429	0.04340
9	0.08237	2.85127	0.03734	0.04363
10	0.07521	2.56711	0.02233	0.03933
11	0.07351	2.31746	0.01383	0.02644
12	0.06885	2.13902	0.00910	0.02677
13	0.07662	1.96043	0.00602	0.01342
14	0.08501	1.81659	0.00420	0.00023
15	0.09748	1.69758	0.00297	0.00000
16	0.09923	1.59027	0.00206	0.00197
17	0.11695	1.49977	0.00148	0.00004
18	0.19996	1.43167	0.00109	0.00006
19	0.17280	1.34942	0.00072	0.00114
20	0.26019	1.28487	0.00050	0.00000
21	0.27998	1.22450	0.00031	0.00342
22	0.27817	1.17116	0.00017	0.09748

Table S16. Best fitted parameters (χ_T, χ_S, τ and α) with the extended Debye model for complex **5** at 0 Oe in the temperature range 3-22 K.

T/ K	χ_S / cm^3 mol^{-1}	χ_T / cm^3 mol^{-1}	τ/s	α
5	0.17303	4.19306	0.00178	0.21533
6	0.13976	3.42969	0.00159	0.20240
7	0.15497	2.97554	0.00155	0.19981
8	0.13471	2.60245	0.00139	0.18935
9	0.13920	2.30408	0.00125	0.16943
10	0.13915	2.03000	0.00105	0.13423
11	0.14509	1.89080	0.00096	0.13427
12	0.12902	1.73417	0.00082	0.12327
13	0.13948	1.60356	0.00071	0.10264
14	0.13822	1.48656	0.00059	0.08432
15	0.13958	1.38624	0.00049	0.06624
16	0.10567	1.31420	0.00040	0.06310
17	0.09058	1.23448	0.00031	0.06229
18	0.13818	1.17040	0.00026	0.04645

19	0.13745	1.10656	0.00020	0.03939
20	0.05241	1.05213	0.00013	0.07814

Table S17. Best fitted parameters (χ_T, χ_S, τ and α) with the extended Debye model for complex **5** at 1500 Oe in the temperature range 8-22 K

T/ K	χ_S / cm^3 mol^{-1}	χ_T / cm^3 mol^{-1}	τ/s	α
6	0.06033	3.20393	0.10010	0.06086
7	0.04381	2.98087	0.05174	0.08477
8	0.03875	2.61352	0.02603	0.07263
9	0.03322	2.32000	0.01463	0.06693
10	0.03382	2.08478	0.00902	0.06285
11	0.03610	1.90837	0.00573	0.05043
12	0.03036	1.73787	0.00391	0.05877
13	0.02924	1.60715	0.00274	0.05730
14	0.03252	1.49479	0.00191	0.04986
15	0.03107	1.39827	0.00137	0.04971
16	0.03714	1.31396	0.00099	0.04180
17	0.05699	1.24243	0.00071	0.03452
18	0.07407	1.17484	0.00050	0.02200
19	0.08499	1.11660	0.00034	0.02227
20	0.12396	1.06715	0.00023	0.00599

Table S18. Energy barriers obtained from the Arrhenius law fitting and Equation 1 of the out-of-phase (χ'') ac susceptibility data under zero dc field.

Relaxation processes	Orbach processes		Raman, QTM and Orbach processes				
	U_{eff}/κ_B (K)	τ_0 (s)	q	C ($s^{-1}\cdot K^{-n}$)	n	U_{eff}/κ_B (K)	τ_0 (s)
3	73.46	5.18×10^{-6}	0.002	8	1.71	90.40	4.20×10^{-6}
4	82.05	5.98×10^{-6}	0.008	7	1.68	95	6.09×10^{-6}
5	68.68	5.66×10^{-6}	0.002	0.24	2.96	70	1.05×10^{-5}

Table S19. Energy barriers obtained from the Arrhenius law fitting and Equation 2 of the out-of-phase (χ'') ac susceptibility data under optimum dc field.

Relaxation processes	Orbach processes		Raman and Orbach processes			
	U_{eff}/κ_B (K)	τ_0 (s)	C ($s^{-1}\cdot K^{-n}$)	n	U_{eff}/κ_B (K)	τ_0 (s)
1	37.64	7.80×10^{-7}	0.045	5.64	39.65	9.79×10^{-7}
2	28.64	1.15×10^{-5}	0.001	1	30.30	9.48×10^{-6}
	152.73.	1.22×10^{-7}	0.005	4.23	160	1.55×10^{-7}
3	157.38	1.26×10^{-7}	0.002	4.40	165.25	1.44×10^{-7}
4	154.79	2.03×10^{-7}	0.001	4.62	175.55	1.46×10^{-7}
5	122.23	5.20×10^{-7}	0.003	4.60	128.27	1.28×10^{-6}